AMS Note 2002-11-03

A proposal for a low energy gamma trigger (algorithm and rates)

Mariusz Sapinski *, Alain Falvard and Agnieszka Jacholkowska
Groupe d'Astroparticules de Montpellier,
University Montpellier II, Place Eugene Bataillon,
34095 Montpellier CEDEX, France

March 25, 2003

Abstract

The studies of the AMS gamma trigger performed in [1] have shown that triggering for photons with energies above 8 GeV in electromagnetic calorimeter is possible and will not enhance substantially the total trigger rate. Trigger criteria (LV1) were based on transverse width of the electromagnetic shower and the total deposited energy. The goal of this study is to investigate a possibility to lower the γ-trigger threshold. This could be obtained by introducing additional trigger conditions and by using additional variables. Detection of photons in energy range from 2 to 8 GeV can be crucial for investigation of Gamma Ray Bursts, supersymmetric Dark Matter halos and for measurement of γ -ray sources.

*contact person, mail: mariusz.sapinski@gamum2.in2p3.fr

Contents

1 Introduction

Alpha Magnetic Spectrometer (AMS) is a high-energy detector to be placed on the International Space Station. The main goal of the AMS is to measure the flux of charged particles and search for antimatter. A measurement of high energy photon flux is also possible. It will be done with two AMS subdetectors: electromagnetic calorimeter and/or tracker. This would allow to investigate astrophysical sources such as: pulsars, blazars, gamma ray bursts, Dark Matter halos and diffuse backgrounds. Energy measurements in ECAL would help to answer a large number of questions discussed in [9].

The triggering on photons in AMS is based on tracker in case of converted photons or on the Electromagnetic Calorimeter (ECAL) for those with no conversion. Here we discuss standalone gamma trigger based only on the ECAL measurements.

The Electromagnetic Calorimeter of AMS is made of lead and scintillator material mounted in a SPACAL structure with a total thickness of 16 radiation lengths and about 0.5 of interaction length. This corresponds to about 16.65 cm of the depth of the ECAL, while its transverse dimensions are $65.8 \times 65.8\ cm^2$.

For trigger purpose only dynode signals of photomultipliers are used, which means that granularity of the ECAL is 36x36 in horizontal (transversal) plane and 9 in vertical (longitudinal) direction. Each PM consists of four anodes which provides fine granularity of 72x72x18.

The aim of this work is to study algorithms which would allow to trigger for gamma with less than 8 GeV of energy deposited in ECAL.

A lower gamma trigger energy threshold would increase the proton trigger rate, due to the large flux of background protons which accounts for more then 99% of the total flux.

The bandwidth connecting AMS detector with earth-based control room is almost already filled with triggers of various types. It is clear that one should aim to provide the average (over orbit) trigger rate not significantly increased when adding the low energy γ trigger.

To evaluate gamma trigger efficiency and trigger rate the efficiency function $\varepsilon_{trig}(E,\theta)$ has been determined in 3 bins of θ angle (ie. angle between z-axis and direction of incident particle) and in 22 bins of energy. This procedure allows to determine the energy and direction of the most "dangerous" protons, in which case it would help to develop the optimal trigger criteria.

The report is organized as follows. First we discuss MC samples used to evaluate the results and the methods of acceptance and trigger rate calculation. Then the results obtained by standard algorithm followed by simple extension of standard algorithm to low energies. Then we discuss optimization of trigger parameters and the new variables, which could be used in the trigger scheme. The overall performance and stability of the proposed scenario is presented. Before concluding, few remarks about longitudinal segmentation are given.

2 Samples

Below, we shortly discuss MC samples generated for this study. Proton and gamma samples were generated with the AMS simulation and reconstruction code version 4.00/5/2 released in March 2002. Electron and helium samples were generated with software version from December 2002. These codes use Geant 3.2 [4]. Simulation (except for electrons) were performed on a farm of 10 dual-processor computers of the Groupe d'Astroparticules de Montpellier.

2.1 Proton sample

A sample of about 8 million protons with kinetic energies from 0.5 to 200 GeV following the spectrum $E^{-2.78}$ (due to generation procedure they are useful above about 1.5 GeV) have been produced. The protons have been generated isotropically on the surface of the box around the detector (Figure 1). Most of the particles generated in this way do not reach ECAL. To keep the generation efficiency on reliable level, events are stored in the ntuple if they deposit a minimal energy in the calorimeter (a deposit of at least 1 MIP is required). In good approximation this is a non-biased sample of protons seen by the calorimeter, relevant for the trigger studies.

The charged trigger conditions were required before applying ECAL trigger. This procedure removes 5% of proton candidates accepted by the γ trigger algorithm. All numbers quoted in this study are therefore corrected for the charged trigger selections.

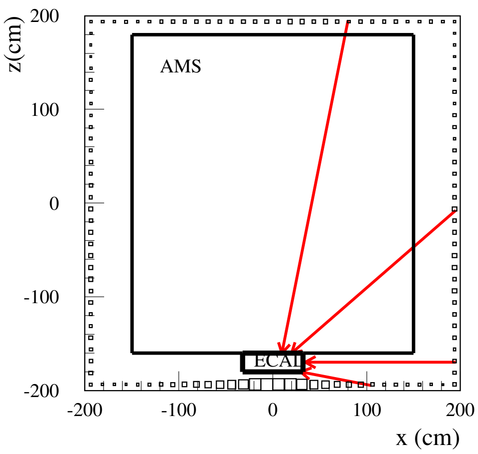

Figure 1: *Positions of generated protons. Events are stored if they give at least 1 MIP (about 120 MeV) signal in the ECAL. Due to the geometry, an excess of events can be observed close to ECAL. To clarify the plot, protons generated on "walls" (planes defined by $y = \pm 200$ cm) have been removed. Red arrows show examples of proton tracks.*

Table 1: Electron fluxes used in trigger rate calculations.

E_{min} (GeV)	E_{max} (GeV)	flux $(m^{-2} \cdot sr^{-1} \cdot s^{-1})$
upward-going		
0.22	0.31	7.60
0.31	0.44	7.00
0.44	0.62	6.17
0.62	0.85	5.15
0.85	1.15	3.05
1.15	1.54	2.46
1.54	2.02	1.93
1.54	2.62	1.58
2.62	3.38	1.33
downward-going		
0.20	0.40	7.00
0.40	1.00	15.0
1.00	2.62	18.0
2.62	3.38	2.91
3.38	4.31	1.68
4.31	5.45	1.01
5.45	6.86	0.62
6.86	8.60	0.39
8.60	10.7	0.24
10.7	13.3	0.15
13.3	16.6	0.10
16.6	20.5	0.06
20.5	25.3	0.04
25.3	31.2	0.03

Another sample of protons has been generated to calculate acceptance of ECAL. This sample was generated in energy bins corresponding to bins from [5], with E^{-1} energy spectrum and in bins of θ, as described later.

2.2 Electron sample

As can be found in [7], the electron and positron fluxes reach maximum in QuasiPolar point of the orbit for downward-going particles (Figure 2b from [7]) and in Equatorial point of the orbit for upward-going particles (Figure 3d from [7]). Electron sample were generated by Stefano di Falco, following the maximal fluxes. The energy bins and flux values used in this note are presented in Table 1.

2.3 Gamma sample

The photons are generated in narrow energy bins at energies from 2 to 120 GeV. They are generated from a plane placed above the detector (z=200 cm). As only photons contained in fiducial volume are interesting here, the following additional selection cuts are imposed:

1. incident angle of the particle $< 23\,\mathrm{deg}$
2. $|x_{z=-140cm}|$ and $|y_{z=-140cm}|$ of the gamma trajectory projected on z=-140 cm smaller then 30 cm (the calorimeter upper surface)
3. $\sqrt{x^2_{z=65cm} + y^2_{z=65cm}}$ of the gamma trajectory projected on z=65 cm smaller then 45 cm (position of the TOF1 and TOF2)

The above conditions select not only gammas from fiducial volume but also allow to avoid gammas in the difficult region (for instance gammas registered near the side of the ECAL, where a substantial transverse leakage spoils the γ reconstruction). Study of such peripheral cases should be done separately.

The primary gammas which were converted in Transition Radiation Detector (about 13% of the generated sample) should be triggered by charged trigger and are not taken into account here.

2.4 Helium sample

Helium was generated in bins of rigidity from Table 1 of [8]. The primary spectrum has been considered here as the geomagnetic cutoff almost does not affect helium nuclei in the QuasiPolar region. The composition of primary flux of helium is: 88.5% of He4 and 11.5% of He3. Here only He4 has been considered.

3 Determination of acceptance

Acceptance and trigger rejection power have been determined in the same θ angle and logarythmic kinetic energy bins. There are 22 bins in energy from 1.54 GeV to 200 GeV, as in the AMS-01 original work [5].

Four bins of θ, where θ is an angle between zenith and a chosen direction, has been defined:

- $0\ deg < \theta_1 < 23\ deg$ (in fiducial volume)
- $23\ deg < \theta_2 < 64\ deg$ (magnet area)
- $64\ deg < \theta_3 < 90\ deg$ (side-going) [1]

[1]due to 20 deg tilt of the AMS the range of this bin can be stretched to 110 deg

- $\theta_4 \ > \ 90 \ deg$ (upward-going)

The total geometrical acceptance of the ECAL is defined by the expression:

$$A_{ECAL} = \int d\Omega \int_{det} dS \cdot \varepsilon_{accept}(\theta, \phi, x, y) \qquad (1)$$

which leads to the differential form:

$$A_{ECAL}(E, \theta, \phi) = \int_{det} dS \cdot \varepsilon_{accept}(\theta, \phi, x, y) \qquad (2)$$

where $\varepsilon_{accept}(\theta, \phi, x, y)$ is an efficiency for particle detection in ECAL. Assuming azimuthal symmetry and a "finite element" approximation we have used the following formula:

$$A_{ECAL}(\Delta E_{kin}, \Delta\theta) = \sum_{ij} \delta S_{ij} \frac{N_{ij}^{meas}(\Delta E_{kin}, \Delta\theta)}{N_{ij}^{gen}(\Delta E_{kin}, \Delta\theta)} = A_{BOX} \cdot \frac{N_{sig}(\Delta E_{kin}, \Delta\theta)}{N_{gen}} \qquad (3)$$

where N_{sig} is number of events accepted by the condition of leaving a minimal signal in ECAL and N_{gen} is number of events generated in the given bin of E_{kin} and θ $(\Delta E_{kin}, \Delta\theta)$. A_{BOX} is acceptance of the box where protons are generated and is equal to 286.7 $m^2 \cdot \ sr$.

Acceptance as a function of kinetic energy is presented in bins of θ on Figure 2. There is a strong dependence on incident proton angle, the geometrical acceptance increases weakly with proton energy.

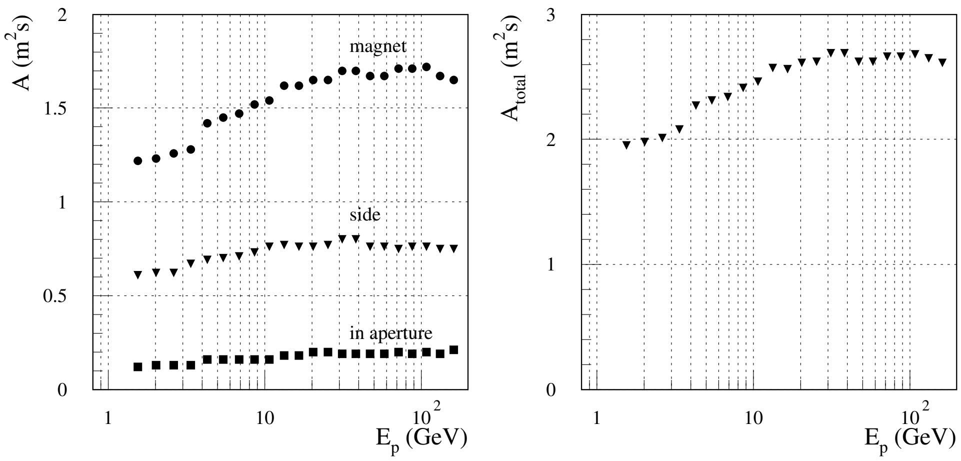

Figure 2: *The ECAL geometrical acceptance for protons as a function of protons kinetic energy in 3 bins of θ (left plot) and the total acceptance when summed up over all θ (right plot).*

4 Particle flux on the orbit

4.1 Particle flux

The proton fluxes used to evaluate trigger rates are taken from [6]. These fluxes correspond to the one measured by AMS-01 mission on STS-91 space shuttle flight. That 10-day long precursor flight took place in June 1998 on space shuttle Discovery.

From these data one can see that above momentum of about 8 GeV proton flux does not depend on the position on the orbit. The high energy protons are of cosmic origin (i.e. they are downward-going in AMS reference frame). Protons with energies below 8 GeV behave differently, in various places of the orbit. The protons in equatorial region are trapped in the magnetic field of the Earth so they arrive, with the same probability, from the upper and the down directions. In equatorial region, where the geomagnetic cutoff is an important factor, the flux is smaller (below the cutoff value) than for higher latitudes.

For high latitudes the low energy proton flux is not affected by geomagnetic cutoff (value of this cutoff for $\Theta_M \approx 1\ rad$ is below 1 GeV), so the flux of upward-going (i.e. trapped) protons is negligible for energies above 1 GeV, but the flux of low energy downward-going protons is much higher than in equatorial region.

Another aspect is solar modulation parameter, which is a parameter used to describe solar activity. During the period when the Sun is active, the solar magnetic field is stronger and shields Earth from low energy cosmic protons. The flux of low energy protons can be suppressed by a factor of 2. AMS-01 data were obtained in period of moderate solar activity, while AMS-02 will fly longer and the during the mission the solar activity minimum will take place. The effect of increase of low-energy proton flux due to this minima is estimated later in this note.

The movement of the particles trapped by the geomagnetic field consists of three components: gyration around magnetic field lines, bouncing (along lines of magnetic field) and drift (east-west direction, depending on the charge). On low orbit gyration leads particles throught regions with various density of the atmosphere. In the lower part particles are absorbed more easily, what leads to East-West asymmetry in flux of charged particles. In this note we use an average flux.

For an altitude of about 400 km above southern part of Atlantic Ocean, there is a region where the magnetic field of Earth is anomalous. This anomaly attracts radiation belts which, in this region, reach altitude of the ISS orbit. Low energy proton flux in South Atlantic Anomaly (SAA) is much larger than in the rest of the orbit. In this note we do not discuss trigger scenario for SAA region, however it is possible, that it will be necessary to switch off gamma trigger when passing through SAA (data taken there by AMS-01 were excluded from standard analysis).

Helium flux is about 2 orders of magnitude smaller than the proton one, but its behavior changes with latitude in the same way.

Below we discuss the trigger rates in three points on the orbit: with the smallest, the middle and the largest geomagnetic latitude. They approximate fluxes are shown in Figure 3.

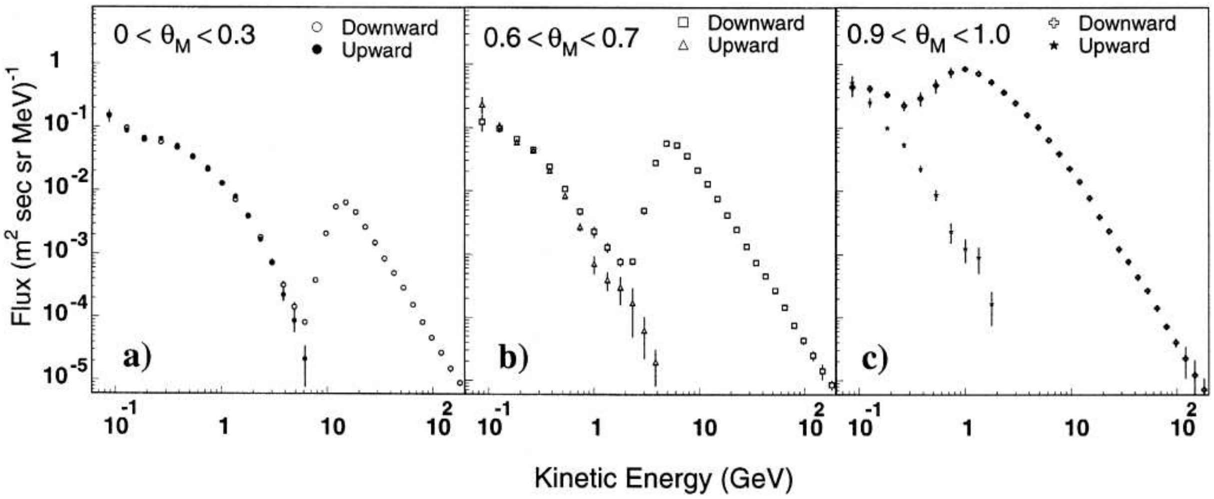

Figure 3: *Proton differential flux in the equatorial (left plot), middle (middle plot) and 'polar' (right plot) regions (from [6]).*

Equatorial point

The equatorial point is a point with geomagnetic latitude $\Theta_M < 0.2\ rad$. Differential flux of protons for this point is presented on the left plot of Figure 3. One may notice that the energy spectrum consists of two parts. The high energy part corresponds to cosmic protons. They are downward-going and the spectrum ends-up at the value of geomagnetic cutoff, which is equal to about 15 GeV for equatorial regions.

The low energy part consists of protons trapped in Earth magnetic field. These protons arrive from all directions. The upward-going part fortunately does not give a significant contribution to the total trigger rate.

Here we calculate trigger rate using the spectrum shown below (we use exact numbers from tables in [6]) and assuming that the detector is not tilted with respect to the horizon.

In Equatorial point of the orbit the flux of upward and downward going positrons is much larger than electrons (Figure 3d from [7]). The influence of this flux on the total trigger rate is evaluated later in this note.

Middle point

The 'middle' point has been chosen as the one with geomagnetic latitude $\Theta_M = 0.5 - 0.6\ rad$. The low energy proton flux increases trigger rates for trigger threshold of 2 GeV, by a factor of 2 with respect to the Equatorial point. The flux as a function of energy is presented on the middle plot of Figure 3.

QuasiPolar point

The 'QuasiPolar' point represents the most distanced point from the equator of the ISS orbit, with geomagnetic latitude $\Theta_M \approx 1\ rad$. In this region few protons are trapped in the Earth magnetic field so the upward-going flux has a limit below 8 GeV. On the other hand, due to much smaller value of the geomagnetic cut-off, the flux of downward-going low energy protons is high (right plot of Figure 3). These protons are mainly responsible for high total trigger rate. Fortunately ISS orbit is such that for about 80% of time the radiation conditions are closer to equatorial than to QuasiPolar ones.

Electron spectra for this point have the following features: upward going flux is negligible above 2 GeV while downward going flux is about 10-100 times smaller then in case of protons (Figure 2b from [7]).

4.2 Calculation of the trigger rate

Trigger rates for protons in this note are calculated from the formula:

$$Rate = \sum_{E_{kin}} \sum_{\theta} A_{ECAL}(E_{kin}, \theta) \cdot \Phi(E_{kin}, \theta) \cdot \varepsilon_{trig}(E_{kin}, \theta) \tag{4}$$

where Φ - differential proton flux on the orbit, A_{ECAL} - ECAL acceptance, and ε_{trig} - trigger efficiency for protons.

The trigger rate for electrons and helium is calculated from the formula:

$$Rate = A_{BOX} \cdot \sum_{E_{kin}} \sum_{\theta} \Phi(E_{kin}, \theta) \cdot \varepsilon_{trig}(E_{kin}, \theta) \cdot \varepsilon_{accept}(E_{kin}, \theta) \tag{5}$$

where ε_{accept} is efficiency of the particle detection. This formula is used to calculate trigger rate for helium and electrons. It has been verified that for protons both approaches give similar results [3].

5 Fast trigger

The AMS level 1 trigger comprises a fast trigger, which should give the information if an event is potentially interesting, within about 200 ns with respect to a particle passing thought the detector. The rest of information needed for level 1 trigger (LV1) requires more time - about $2\mu s$.

The fast trigger uses a dynode analog sum which is proportional to the total energy deposited by a particle in ECAL. In the simulation the analog sum corresponds to E_{tot}. This variable leads to a quite high frequency of the fast trigger. The criterium $E_{tot} > 2\ GeV$ gives fast trigger rate between 100 Hz in equatorial AMS position and 460 Hz in the QuasiPolar point of the orbit. For E_{tot} calculated without the first superlayer (as in algorithm proposed later in this note) fast trigger rate for QuasiPolar point of the orbit is 405 Hz. The trigger condition $E_{tot} > 8\ GeV$ gives the orbit independent rate of about 35 Hz which decreases to about 30 Hz without use of the first superlayer.

6 Optimization and performances

In the original work [1] the gamma-trigger for AMS detector was based on cut on total energy deposited in calorimeter and transverse width of the shower. The transverse width of the cascade is expressed in number of PM hits projected into xy-plane: $N_x + N_y$. There are two ways of calculating $N_x + N_y$:

- take a cell as fired if a signal from this cell is larger than some threshold E_{thr}^{PM}. Such a fired cell gives the whole column being included in $N_x + N_y$. The results depends on E_{thr}^{PM} and in this note we used value of 100 MeV, which seems to be optimal [1];

  or

- sum signals from PMs in a column and verify if this sum is larger than some threshold E_{thr}. The threshold can be different for columns in x and y directions, because there are 4 even and 5 odd superlayers, ie. columns contain 4 PMs in x-direction and 5 in y-direction. It has been found that results are similar for both methods of $N_x + N_y$ calculation if E_{thr}=120-160 MeV for x and 150-200 MeV for y-columns. The correct, from implementation point of view, way to calculate $N_x + N_y$ is putting the threshold on sum of the signals in a column.

The cuts used in [1] (see Section 6.1) give almost 100% efficiency for gamma above 8 GeV [2] and about 10-15 Hz of proton rate [3].

6.1 Standard algorithm

In the standard gamma trigger algorithm, the following set of four conditions have been proposed [1]:

[2]The gamma sample used to evaluate the efficiency has been biased by pre-trigger cuts.

[3]Isotropic flux is assumed, while in reality the shadow of Earth shields ECAL form upward-going protons.

- trigger condition 1: 8 $GeV < E_{tot} <$ 18 GeV and $N_x + N_y <$ 10 ([4]), or
- trigger condition 2: 18 $GeV < E_{tot} <$ 48 GeV and $N_x + N_y <$ 13, or
- trigger condition 3: 48 $GeV < E_{tot} <$ 100 GeV and $N_x + N_y <$ 16, or
- trigger condition 4: $E_{tot} >$ 100 GeV

Cuts based on transverse parameters of the cascade ($N_x + N_y$) have been chosen to reject background particles coming from the side of the ECAL, which is not shielded and which does not contain veto detectors. In this note we will call this algorithm STD, if threshold is imposed on a sum of the signals in a column. The algorithm with 100 MeV threshold per PM (as in original work [1]) is called STD*. STD algorithm with $E_{thr} = 160 - 200\ MeV$ for x and y-columns respectively gives results close to STD* algorithm.

The STD algorithm gives γ trigger efficiency above 98% for photons above 9 GeV (see left plot of Figure 4). Photons with energies above 20 GeV are triggered with probability of 100%. Trigger rate due to protons is about 5 Hz (see Table 2) and does not depend on the position on the AMS orbit [5].

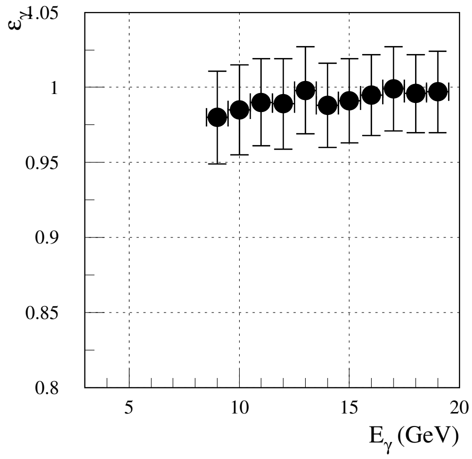

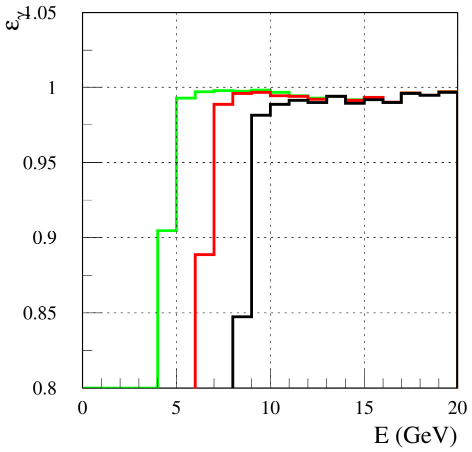

Figure 4: *Photon trigger efficiency as a function of photon energy for STD trigger with energy threshold for each channel E_{thr} set to 160 MeV for x and 200 MeV for y-column (left plot). On the right plot an effect of simple lowering trigger threshold is presented.*

---

[4]There is a mistype in the note suggesting that this condition is: $E_{tot} > 8\ GeV$ and $E_{total} < 18\ GeV$ and $N_x + N_y < 9$, the same concerns trigger condition 2 and 3

[5]This result is different than in [1], and the difference originates mainly from the fact that protons used in [1] were simulated from around the ECAL and not whole the AMS detector.

Table 2: Proton trigger rates for algorithms STD with energy threshold for each channel E_{thr} set to 160 and 200 MeV in x and y-columns respectively. STD* algorithm uses threshold on PM, instead of threshold on column.

algorithm	E_{thr} (GeV)	trigger rate		
		R_{eq} (Hz)	R_{mid} (Hz)	R_{qp} (Hz)
STD* [1]	8	5	5	5
STD	8	5	5	5
STD	6	9	12	12
STD	4	20	42	65
STD	2	40	103	311

6.2 Extension to low energies

The most simple extension to lower energies is just a lower energy threshold. This gives very good trigger efficiencies (see right plot of Figure 4) but as shown in Table 2 the trigger rates are rather high. It is clear that trigger rate above 300 Hz is not acceptable for the ECAL trigger. Energy threshold of 2 GeV cannot be reached without additional criteria. Before adding new criteria, the basic parameters such as E_{thr} per channel and $N_x + N_y$ cuts should be optimized.

6.3 Optimization of E_{thr} per column

Each columns of ECAL is composed of 4 x-direction PMs or 5 y-direction PMs. From electronic point of view it is recommended to use the same threshold value for x-columns and for y-columns. Moreover, as the first superlayer does not collect significant amount of the energy of photons, the information from this superlayer could be discarded in the trigger scheme. In the algorithm discussed below all variables are calculated from energy deposits in superlayers 2 to 9.

The optimal E_{thr} value is the one which gives maximal separation between $N_x + N_y$ distribution for protons and for photons. Figure 5 shows $N_x + N_y$ distributions for protons and gammas leaving energy deposit $E_{tot} = 1.5 - 2.5\ GeV$ in ECAL. Left plot shows distributions for $E_{thr} = 80\ MeV$ and the right one for $E_{thr} = 120\ MeV$. Lower threshold gives better separation. However, due to the characteristics of the comparators which are used in the trigger circuits, this threshold should not be lower than a certain value. So, the useful range is 80-120 MeV.

The low value of E_{thr} makes also the trigger efficiency dependent on the energy. The decrease in some regions correspond to step transitions and could be overcome by introducing additional conditions.

Here, the value chosen of E_{thr} is 90 MeV due to a compromise between the simplicity of the algorithm and its performance. This value is also conservative, eg.

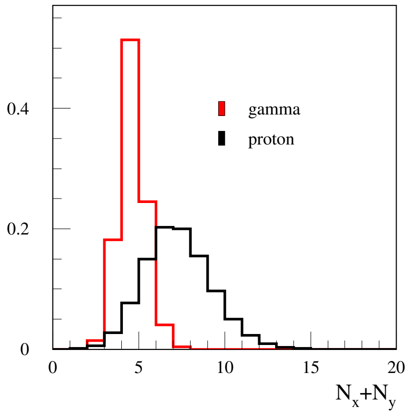

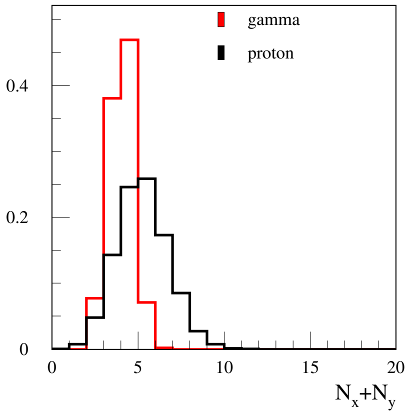

Figure 5: *$N_x + N_y$ distributions for protons and photons leaving $1.5\ GeV < E_{tot} < 2.5\ GeV$ for $E_{thr} = 80\ MeV$ (left plot) and $E_{thr} = 120\ MeV$ (right plot).*

one can study more performant algorithms, which also would be more difficult to implement in the electronic scheme.

6.4 Optimization of $N_x + N_y$ cut

In this subsection we discuss the number and structure of trigger conditions.

The value of the $E_{thr} = 90\ MeV$ has been chosen from previously described optimization procedure. The choice of energy steps of the trigger scheme should ensure the trigger efficiency to be above 95% in the whole energy range[6].

Generally larger number of steps allow to distinguish more precisely photons from protons. On the other side too many steps in energy would make difficult the trigger implementation. In fact increasing number of steps would lead to a large number of trigger conditions for low energy, with step size of about 1-2 GeV.

The number of trigger conditions has been chosen to be 5, plus the very high energy criterium where the cut on $N_x + N_y$ is no longer used. The following set of trigger conditions may lead to the minimal trigger rate in QuasiPolar point of the orbit:

- trigger condition 1: $2\ GeV < E_{tot} < 4\ GeV$ and $N_x + N_y < 7$, or
- trigger condition 2: $4\ GeV < E_{tot} < 8\ GeV$ and $N_x + N_y < 9$, or
- trigger condition 3: $8\ GeV < E_{tot} < 18\ GeV$ and $N_x + N_y < 11$, or

[6]At the trigger energy threshold of 2 GeV trigger efficiency is mostly driven by the energy resolution and is equal to about 50%.

- trigger condition 4: 18 $GeV < E_{tot} <$ 48 GeV and $N_x + N_y <$ 15, or
- trigger condition 5: 48 $GeV < E_{tot} <$ 100 GeV and $N_x + N_y <$ 19, or
- trigger condition 6: $E_{tot} >$ 100 GeV

The proposed trigger scheme is presented in Figure 6, where the γ and proton populations are displayed as a function of $N_x + N_y$ and E_{tot}.

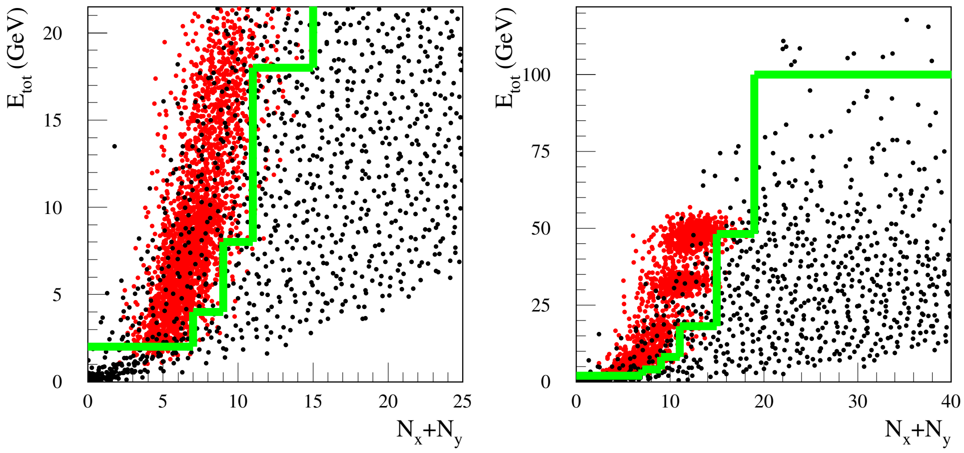

Figure 6: *Trigger schemes for low energies (left plot) and for high energies (right plot). Red dots stand for gammas while the black ones for protons.*

6.5 N_{block} criterium

For low values of the deposited energy the distributions of $N_x + N_y$ for gamma and for protons overlap. The low energy side going protons tend to fire low number of columns as in case of photons. Fortunately photons are likely to fire neighbor columns while the protons coming from the side leave columns with signal in between being below threshold E_{thr}. These cases are illustrated in Figure 7.

The variable N_{block} is defined as a number of blocks of fired columns in x and in y separated by an empty gap. For instance in Figure 7, N_{block} for gamma is equal to 1 and for protons it is equal to 2. But as in this Figure only one-side columns are shown one should expect N_{block} equal to at least 2 (one in each direction).

The distributions of N_{block} for protons and photons is shown in Figure 8. The preferable cut to select photons is $N_{block} \leq 2$. This cut works well for low energies only, so it is used as an additional criterium for the lowest-energy condition. The N_{block} variable is weakly correlated with $N_x + N_y$ and gives additional rejection factor of about 3.

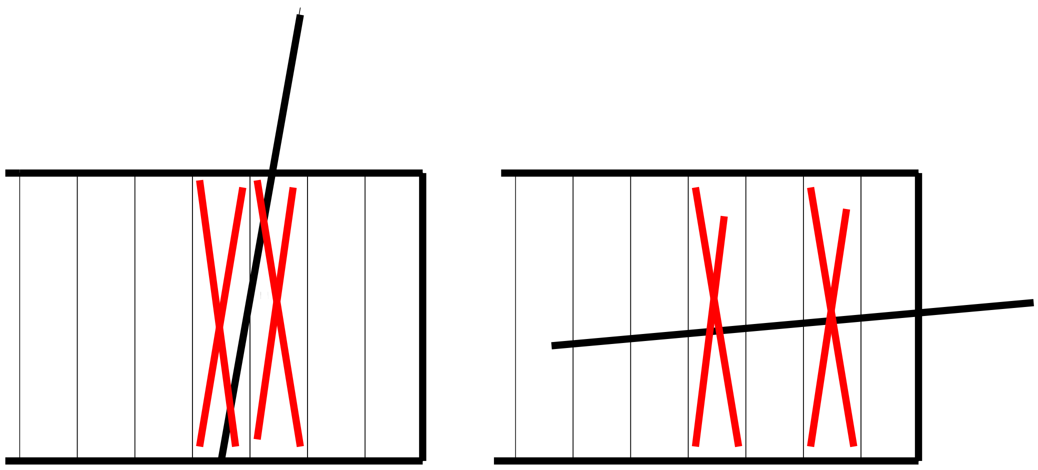

Figure 7: *An example of low energy photon (left plot) and proton (right plot) behavior in ECAL.*

The final proposed set of trigger conditions is the following:

- **trigger condition 1:**
  $2\ GeV < E_{tot} < 4\ GeV$ **and** $N_x + N_y < 7$ **and** $N_{block} \leq 2$
- **trigger condition 2:**
  $4\ GeV < E_{tot} < 8\ GeV$ **and** $N_x + N_y < 9$**, or**
- **trigger condition 3:**
  $8\ GeV < E_{tot} < 18\ GeV$ **and** $N_x + N_y < 11$**, or**
- **trigger condition 4:**
  $18\ GeV < E_{tot} < 48\ GeV$ **and** $N_x + N_y < 15$**, or**
- **trigger condition 5:**
  $48\ GeV < E_{tot} < 100\ GeV$ **and** $N_x + N_y < 19$**, or**
- **trigger condition 6:**
  $E_{tot} > 100\ GeV$

6.6 Effect of the energy smearing

In the present simulation, the dynode energy is represented by a sum of energies of the four anodes. This is an optimistic approximation. Energy resolution of an anode signal is:

$$\frac{\sigma(E)}{E} = \frac{10\%}{\sqrt{E(GeV)}} \oplus 2.7\% \tag{6}$$

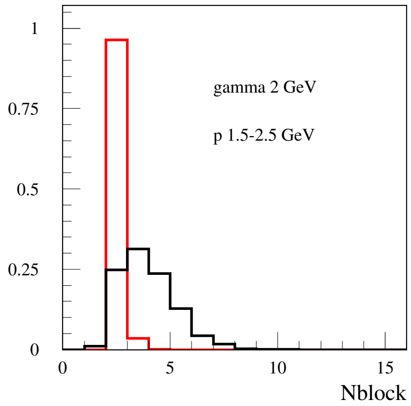

Figure 8: *Distribution of N_{block} variable for photons of 2 GeV and for protons which leave $E_{tot} = 1.5 - 2.5$ GeV energy deposit in ECAL.*

while for dynode it is equal to (as measured in the beam test):

$$\frac{\sigma(E)}{E} = \frac{16\%}{\sqrt{E(GeV)}} \oplus 4\% \tag{7}$$

To get the dynode resolution [7] the energy has been smeared by an energy-dependent factor. In the left plot of Figure 9 one can see energy resolution for 2 GeV photons for anode signal (dashed line) and for dynode signal (solid line). On the right plot the difference in trigger efficiency due to additional smearing is presented for trigger scheme. This smearing affects trigger efficiency for energies below 4 GeV (right plot of Figure 9), and for instance the trigger efficiency for 3 GeV photons falls down from 98.9% with anode resolution to 98.7%. This additional energy smearing changes also slightly the trigger rate, and for QuasiPolar point of the orbit, trigger rate changes from 35 Hz to 37 Hz.

6.7 Overall performance

The algorithm discussed above provides γ -trigger efficiencies as a function of energy as presented in Table 3. This efficiencies as a function of energy are also shown in the left plot of Figure 10. **The γ -trigger efficiency is above 90% for photons with energies above 2.5 GeV.**

A total trigger rate for protons, given by low energy algorithm is about 37 Hz in QuasiPolar point of the orbit and 10 Hz in Equatorial point. The trigger rate in three bins of θ are presented in function of energy on the right plot of Figure 10.

[7] In the new version of software the dynode signal is simulated.

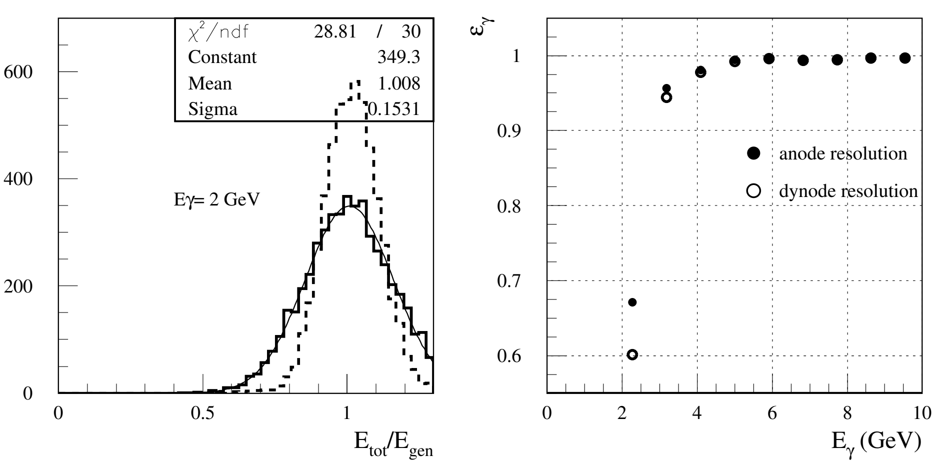

Figure 9: *Energy smearing: effect on the quality of energy reconstruction of photons with energies 2 GeV (left plot) and on trigger efficiency (right plot).*

Proton rates are estimated for AMS-01 flux, which were measured during a relatively active Sun period. For solar modulation parameter as low as 500 MV the maximal trigger rate would raise up to about 50 Hz. The trigger rate due to upward-going protons is very small (about 1 Hz in Equatorial point of the orbit).

Electron flux is the most intense in QuasiPolar region for downward-going electrons and in Equatorial region for upward-going electrons. The additional trigger rate due to electrons is between 1 Hz in Equatorial region and 2 Hz in QuasiPolar.

The trigger rate due to the helium flux is about 12 Hz in the QuasiPolar region. About 8 Hz comes from helium nuclei with rigidity between 1.58 and 2.29 GV. This part of the spectrum is below geomagnetic cut-off so the helium rate decreases very strongly for low latitudes.

As conclusion the total trigger rate (protons+helium+electrons) is predicted to be 50 Hz for active sun period and would raise to about 90 Hz for the low solar modulation parameter period.

6.8 Stability of the algorithm

In this section some points concerning stability of the algorithm are verified.

On the left plot of Figure 11 the photon trigger efficiency and proton trigger rate are shown as a function of threshold on energy in a column - E_{thr}. Variation of this threshold by 10% would lead to 2% variation of trigger efficiency for photons of 2.5 GeV and 25% variation of trigger rate.

On the right plot of Figure 11 photon trigger efficiency as a function of value of $N_x + N_y$ cut for the first trigger condition is presented. For the nominal value of $N_x + N_y$-cut equal to 7 we are at the plateau of efficiency for photons of 2 and 2.5 GeV. However for 4 GeV the working point being $N_x + N_y$=7, we are at the edge of the stability plateau (deterioration of efficiency is at the level of 1%). The

Table 3: Photon trigger efficiency for low energy algorithm. Two groups of photons are selected: with incident angle below 10 deg and with incident angle between 10 and 20 deg. In both cases photons are in fiducial volume of the AMS.

E_γ (GeV)	ε_γ	
	0-10 deg	10-20 deg
2	0.49	0.47
2.5	0.90	0.89
3	0.96	0.95
4	0.98	0.96
5	1.00	1.00
8	0.99	0.99
10	1.00	1.00
20	1.00	1.00
50	1.00	1.00
100	1.00	1.00

variation of the $N_x + N_y$-cut by +1 unity does not change significantly the trigger efficiency however it would increase the proton trigger rate by about 25%. Variation of the $N_x + N_y$-cut by -1 unity would affect trigger rate for 2.5 and 4 GeV photons and would decrease the proton trigger rate by 25%.

7 Use of the longitudinal profile

The trigger algorithms STD and LOW take into account only the transverse profile of the electromagnetic shower and the total energy deposited in the calorimeter. The longitudinal profile of the shower still carries information which can be used to distinguish between hadronic and electromagnetic cascades. Here a method to extract this informations is described.

The most complete information about longitudinal profile of electromagnetic shower is contained in the variables [10]:

$$\frac{\beta}{\alpha} = \frac{1}{\bar{s}} \quad and \quad \frac{1}{\alpha} = \frac{\bar{s^2} - \bar{s}^2}{\bar{s}^2}, \tag{8}$$

where: $\bar{s} = \Sigma s_i E_i / E_{total}$, $\bar{s^2} = \Sigma s_i^2 E_i / E_{total}$ and s_i is the depth (in radiation length) of the i-th longitudinal segment of the calorimeter.

In case of an electromagnetic shower, a gaussian distribution with $\sigma \sim 1$, is expected for the following variables:

$$\frac{\frac{\beta}{\alpha} - < \frac{\beta}{\alpha} >}{\sigma(\frac{\beta}{\alpha})} \quad and \quad \frac{\frac{1}{\alpha} - < \frac{1}{\alpha} >}{\sigma(\frac{1}{\alpha})}, \tag{9}$$

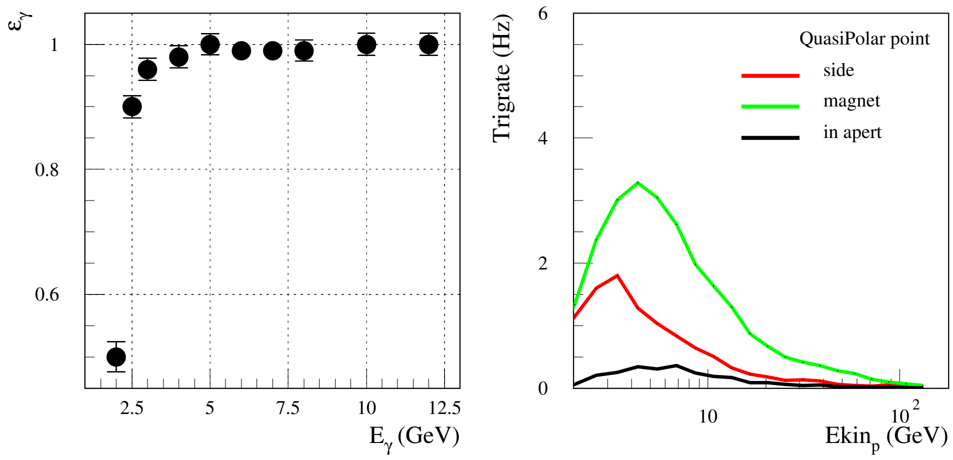

Figure 10: *Left plot: trigger efficiency for low energy photons. Right plot: proton trigger rate in quasi-polar region in various Θ_M bins as a function of proton energy. Every point corresponds to bin of kinetic energy as described in text.*

where $\frac{\beta}{\alpha}$, $\sigma(\frac{\beta}{\alpha})$, $\frac{1}{\alpha}$ and $\sigma(\frac{1}{\alpha})$ are parametrized as a function of photon energy.

Unfortunately, the implementation of this algorithm would make the scheme complicated and probably unrealistic.

Also the algorithm which provides β/α and $1/\alpha$ variables is time consuming.

8 Summary and conclusions

The results presented in this note show that the low energy trigger could be proposed as a simple algorithm in AMS. It has been shown in this Note, it is possible to keep ECAL-gamma trigger rate below 50 Hz in case of a 2 GeV energy threshold. The efficiency of such a trigger is above 95% already at 2.5 GeV (0.5 GeV above the trigger threshold).

It should be emphasized that an adjustable low energy threshold would be very useful due to large variations of low energy particles flux in the orbit.

The proposed scenario with two additional transverse Criteria and cut on N_{block} variable is quite conservative and is already sufficient to keep low trigger rate with high trigger efficiency for QuasiPolar point of the orbit. At present level of studies the longitudinal condition is not recommended, because it would lower significantly the trigger efficiency.

In conclusion, the presented scheme allows to access the physics subjects discussed in the introduction of this note.

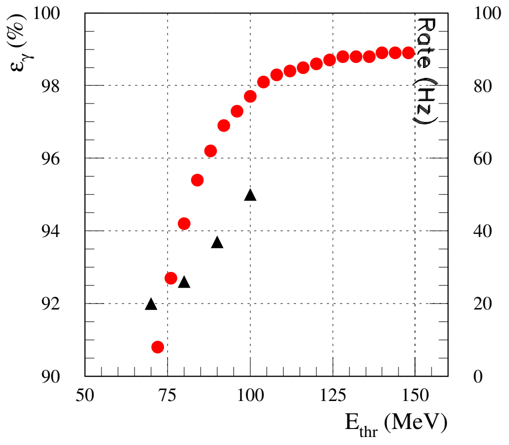

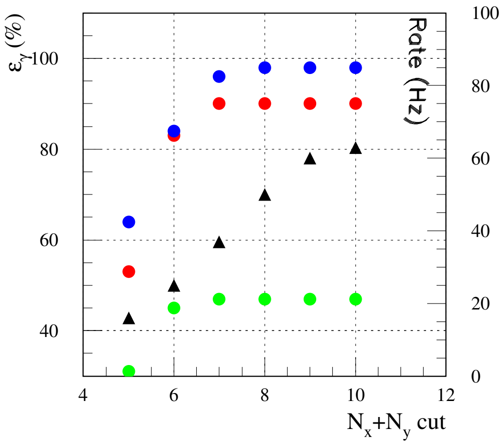

Figure 11: *Left plot: photon trigger efficiency and as a function of threshold on column signal for photons of 2.5 GeV (red dots) and a corresponding trigger rate (black triangles). Right plot: photon trigger efficiency for photons of 2(green dots), 2.5(red dots) and 4(blue dots) GeV and trigger rate (black triangles) as a function of* $N_x + N_y$*-cut.*

9 Acknowledgments

We would like to thank all colleagues from the AMS collaboration for their help. Let me only mention some of them: Corinne Goy who helped us to start working with the AMS software, Sylvie Rosier-Lees who found a lot of time to explain us the technical aspects of the ECAL trigger, Vitaly Choutko, the author of a large part of the software and Eugeni Choumilov, who has implemented the trigger algorithms in AMS simulation software. We would like also to thank Catherine Adloff, Stefano di Falco and Graziano Venanzoni for fruitful discussions. Finally we thank Frederic Piron and Marco Incagli for careful reading of our Note and Michele Bourgeaut for the help she gave us in the MC simulations.

References

[1] C. Goy, S. Rosier-Lees, "Studies for a stand-alone photon trigger using the Electromagnetic Calorimeter", AMS Internal Note.

[2] V. Choutko, G. Lamanna, A. Malinin, "AMS02 Background Studies for Positrons and γ rays", Trento Workshop, October 30, 2001

[3] Catherine Adloff, private communication

[4] R. Brun *et al.*, GEANT 3, CERN DD/EE/84-1 (Revised 1987)

[5] The AMS Collaboration, "Cosmic Protons",
Phys. Lett. **B490** (27-35).

[6] The AMS Collaboration, "Protons in Near Earth Orbit",
Phys. Lett. **B472** (215-226)

[7] The AMS Collaboration, "Leptons in Near Earth Orbit",
Phys. Lett. **B484** (10-22)

[8] The AMS Collaboration, "Helium in Near Earth Orbit",
Phys. Lett. **B490** (193-202)

[9] R. Battiston et al., "The Gamma Ray Detection Capabilities of the Alpha Magnetic Spectrometer", astro-ph/9909432

[10] PDG booklet